Molecular Dynamics Modeling of the Radial Heat Transfer from Silicon Nanowires

Igor Bejenari[a,b], Alexander Burenkov[a], Peter Pichler[a,c], Ioannis Deretzis[d], Antonino La Magna[d]
[a]Fraunhofer Institute for Integrated Systems and Device Technology IISB, Erlangen, Germany
[b]E-Mail: igor.bejenari@iisb.fraunhofer.de
[c]Chair of Electron Devices, University of Erlangen-Nuremberg, Erlangen, Germany
[d]CNR-IMM, Catania, Italy

***Abstract*—Thermal transport in radial direction in Si nanowires embedded into amorphous silicon dioxide has been studied using nonequilibrium molecular dynamics simulations. For comparison, we also considered the axial heat transfer. For Si nanowires with a radius of 2.6 nm, both radial and axial thermal conductivities were found to be about independent of the SiO_2 thickness ranging from 1 nm to 3 nm. The radial thermal conductivity of the Si core and of the covering SiO_2 material are similar and nearly equal to 1 $W \cdot K^{-1} \cdot m^{-1}$. Thermal resistances for the heat transfer from uniformly heated nanowires in radial direction are by a factor of 3 to 4 lower than those for the heat transfer in axial direction.**

Keywords—heat transport, thermal conductivity, nanowire, Molecular Dynamics (MD)

I. Introduction

Silicon nanowires build the basic structure for the next generations of CMOS transistors. In such structures, because of phonon confinement and boundary scattering, the effective thermal conduction is strongly reduced. This poses a limiting factor for many aspects of their application as devices but also for their fabrication via processing steps with low thermal budget like laser annealing. The transport of heat within and from the nanowires to their environment goes in two directions: First, along the wire to the metallic source and drain contacts and, second, in radial direction through the walls of the nanowire and the surrounding dielectric layers to the gate electrode or to other parts of the integrated circuit. The heat transport along the nanowire axis was studied in the literature both experimentally [1] and by simulations [2]. The radial heat transport, on the other hand, has been less addressed and is not well quantified [3]. However, in our earlier work [4] on SOI-FETs we found that it makes an important contribution to the total heat dissipation and we expect similar effects for nanowire FETs.

II. Nonequilibrium Molecular Dynamics Simulations Method

In this work, we investigated nanoscale heat transfer by means of non-equilibrium molecular dynamics (NEMD) simulations exploiting free available software LAMMPS [5], stable version (3 Mar 2020). The Tersoff potential was used to define the structural properties of the Si and SiO_2 atomic systems [6]. In the simulations, the system was first equilibrated in the isobaric-isothermal (NPT) ensemble, then in the canonical (NVT) ensemble. Next, a heat flux was imposed on the system. Finally, when the system has reached a steady state, the temperature gradient between the heat source and sink was calculated as system's response. Thermally grown silicon dioxide as used in electronic technology is amorphous. In this work, the respective atomic structure was created by heating the SiO_2 beyond the melting temperature followed by rapid cooling-down [7].

For the study of the radial heat transport, we use atomic structures like the one shown in Fig. 1. The cylindrical Si nanowire with a length L_{Si} of 10 nm and a radius ρ_{Si} of 2.6 nm is surrounded by amorphous silicon dioxide with thicknesses t_{ox} of 1, 2, and 3 nm. Two different cylindrical heat sources, co-axial with the wire structure, with radii of 0.4 and 2.6 nm and powers of 21.7 and 62.5 $eV \cdot ps^{-1}$, respectively, were used for heat generation. In the first case, this corresponds to a heat source in the structure core, while in the second case the whole Si part of nanowire is heated uniformly. To establish a steady state, a heat sink of equal power was placed on the surface of the structure.

For the study of the heat transport in the direction along the nanowire, we used atomic structures like the one shown in Fig. 2. Here, the heat source with a power of 15 $eV \cdot ps^{-1}$ is uniformly distributed over the silicon part. The left and right lids of the silicon cylinder are covered by a thin layer of silicon dioxide to create a similar material topology for the longitudinal heat transport as it is for the radial one. Two heat sinks with thicknesses of 0.5 nm and a total power of -15 $eV \cdot ps^{-1}$ are located on the external surfaces of the silicon dioxide layers, which are perpendicular to the nanowire axis. The molecular dynamics simulation box indicated by the black lines in Fig. 1 and Fig. 2 defines the borders on which periodic boundary conditions were set-up.

To validate our method, we have simulated the heat conduction along a Si nanowire with a size of 27×27×81 Å. It resulted in a thermal conductivity of 1.75 $W \cdot K^{-1} \cdot m^{-1}$ which is in perfect agreement with the value of 1.8 $W \cdot K^{-1} \cdot m^{-1}$ calculated at 300 K in [2] under the same conditions.

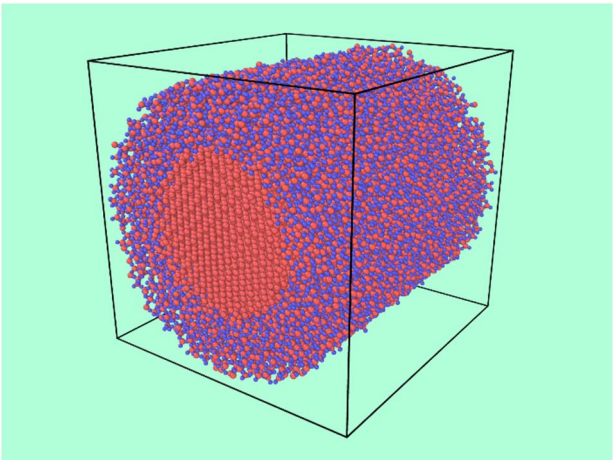

Fig. 1. Atomic arrangement for the study of the radial heat transport in a cylindrical silicon nanowire with a length of 10 nm and growth direction <100>. Radius of the silicon nanowires is 2.6 nm, the nanowire side wall is covered by silicon dioxide with a thickness 2 nm.

The research leading to these results has received funding from the European Union's Horizon 2020 research and innovation programme under grant agreement No. 871813 MUNDFAB.

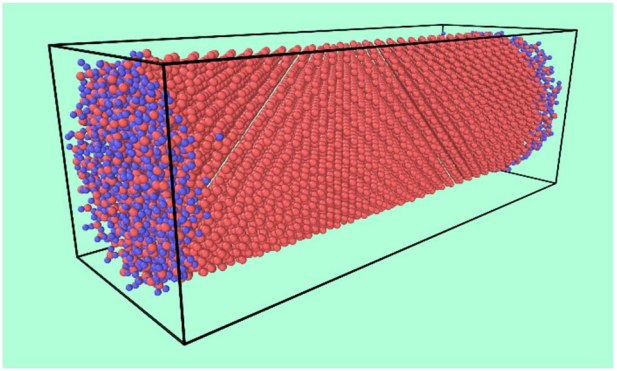

Fig. 2. Atomic arrangement for the study of the axial heat transport in a cylindrical silicon nanowire with a length of the silicon part of 14 nm. Again, the axis of the nanowire corresponds to the <100> crystal direction. The radius of the silicon nanowire is 2.6 nm, top and bottom of the silicon cylinder are covered by silicon dioxide slabs with a thickness 1 nm.

III. Heat Transfer from Locally Heated Silicon Nanowires

As demonstrator, we address exemplarily the important case of silicon nanowires clad with silicon dioxide as shown in Fig. 1 and variants made entirely of silicon dioxide. For a numerical example, silicon nanowires with a diameter of 5.2 nm and a length of 10 nm surrounded by silicon dioxide with thicknesses of 1, 2, and 3 nm have been chosen.

Fig. 3 shows the stationary temperature distribution along the nanowire radius for the nanowires like the one shown in Fig. 1 but with different thicknesses of the oxide. The heat transport was calculated in radial direction for the cylindrical heat source with a radius of 0.4 nm and a power of 21.7 $eV \cdot ps^{-1}$. Please note that the radius scale in all the temperature distribution figures is logarithmic, because the classical macroscopic theory of heat conduction in core-shell cylindrical structures of homogeneous materials predicts a linear dependence in this coordinate system outside the heat sources. The temperature profile has been obtained by averaging the data set of temperatures from 0.6 to 1 ns. As can be seen in Fig. 3, the calculated temperature distribution exhibits several about linear parts that have different slopes in different radii ranges. This is due to the dependence of the phonon properties on the material, on the radius of the wire, and on the oxide thickness.

Fig. 4 shows similar calculations for mono-material nanowires of crystalline silicon or amorphous SiO_2. In comparison to Fig. 3, the temperature distribution in the crystalline silicon nanowire has a higher maximum temperature, lower minimum temperature and about three regions with different slopes. This is due to the phonon boundary scattering and Umklapp phonon scattering at high temperature.

In the amorphous silicon dioxide nanowire, a more smooth temperature distribution is observed predominately because of a relatively small phonon mean free path and, therefore, negligible phonon size quantization effect.

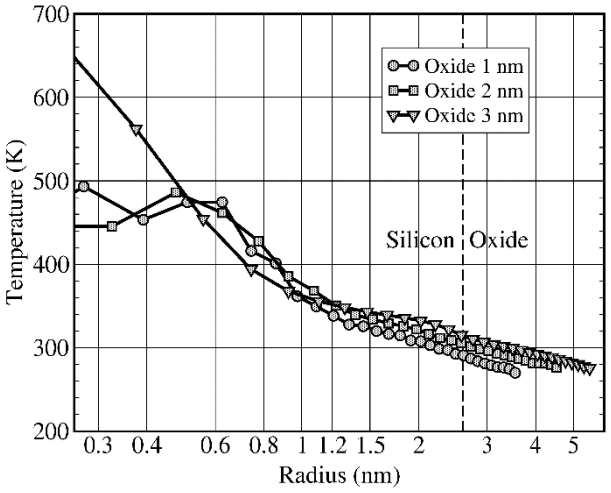

Fig. 3. Temperature distribution as a function of the radius from the axis of the cylindrical nanowire. The radius of the silicon nanowire is 2.6 nm, its cylindrical surface is covered by silicon dioxide with thicknesses of 1, 2, or 3 nm as indicated in the legend. A heat source with a power of 21.7 $eV \cdot ps^{-1}$ is distributed in the inner Si core with a diameter of 0.8 nm. NEMD simulations were performed for 1 ns.

The temperature difference between the maximum and minimum temperatures in these distributions is proportional to the radial thermal resistance. For different materials or material combinations, both the radial thermal conductivity and the thermal resistance were calculated using Fourier's law considering different regions with the constant temperature gradient, see Table I and Table II. We have estimated in Table I also the effective radial interface thermal resistance considering the temperature difference across the smooth Si-SiO_2 interface region with a thickness of $\Delta\rho \sim 0.3$ nm This value is small, because the thermal conductivities in Si and SiO_2 nanowire parts are similar. In addition, due to the atom relaxation, the atomic structure is gradually changing between the two adjacent materials. Therefore, the phonon modes are smoothly changing across the interface resulting in a relatively large phonon spectra overlap.

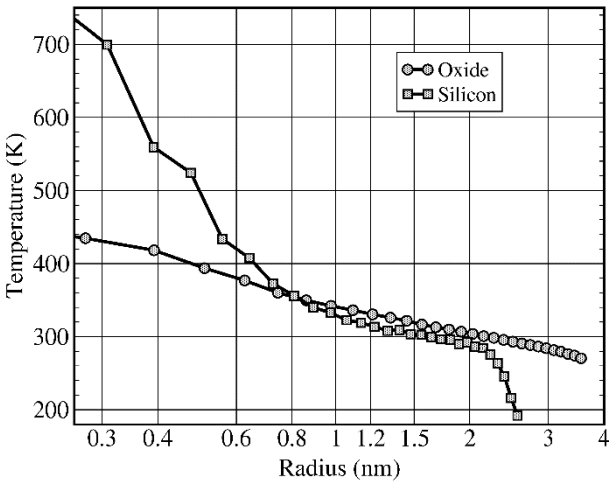

Fig. 4. Temperature distribution as a function of the radius from the axis of cylindrical c-Si and a-SiO_2 nanowires. The radius of the silicon nanowire is 2.6 nm, the one of the silicon dioxide nanowire is 3.6 nm. The heat source with a power of 21.7 $eV \cdot ps^{-1}$ is distributed in the inner nanowire core with a diameter of 0.8 nm. NEMD simulations were performed for 1 ns.

TABLE I. RADIAL THERMAL RESISTANCES
(10 NM LENGTH, 0.4 NM SOURCE RADIUS)

Radial Oxide thickness	Radius (nm)	R^*_{th} (10^{+7} K· W^{-1}) linear part / whole radius	$R_{th,\ interface}$ (10^{+7} K·W^{-1}) from Fourier Law
No oxide	ρ_{Si} = 2.6	0.785 / 17.7	-
1 nm	ρ_{Si} = 2.6	1.47 / 5.02	0.126
2 nm	ρ_{Si} = 2.6	1.82 / 5.24	0.193
3nm	ρ_{Si} = 2.6	2.09 / 12.7	0.346
Oxide only	ρ_{SiO2} = 3.6	1.60 / 5.39	-

TABLE II. RADIAL THERMAL CONDUCTIVITIES
(10 NM LENGTH, 0.4 NM SOURCE RADIUS)

Radial Oxide thickness	Radius (nm)	κ_{Si} (W·K^{-1}·m^{-1})	$\kappa_{Si\text{-}ox}$ (W· K^{-1} ·m^{-1})	κ_{ox} (W·K^{-1}·m^{-1})
No oxide	ρ_{Si} = 2.6	1.05	-	-
1 nm	ρ_{Si} = 2.6	1.10	1.03	0.839
2 nm	ρ_{Si} = 2.6	1.03	1.04	1.18
3nm	ρ_{Si} = 2.6	1.09	1.10	1.12
Oxide only	ρ_{SiO2} = 3.6	-	-	1.04

IV. HEAT TRANSFER FROM UNIFORMLY HEATED SILICON NANOWIRES

A uniform heating of a silicon nanowire is a typical case in many technical applications. For example, in case of laser processing, the light is absorbed mainly in the silicon while the silicon dioxide remains unheated as long as the silicon dioxide is transparent for the chosen wavelength of light. Also in nanowire CMOS transistors, heat is generated in the silicon only because the oxide is electrically not conducting. In this section, we consider the heat transfer from uniformly heated cylindrical silicon nanowires. We compare the heat transport in two directions, radial transport through the sidewalls of the nanowires and axial transport along the nanowires through the end lids.

In the case of radial heat transport, we varied the thickness of the silicon oxide layers that enwrap the silicon nanowire. In CMOS technology, this would mean a variation of the gate oxide thickness of the nanowire transistors. For the heat source power of 65.2 eV·ps^{-1}, distributed uniformly in the silicon part of the nanowire, the resulting temperature distribution along the radius from the nanowire axis is shown in Fig. 5. Because of the periodicity of the simulation setup in the axial direction and the uniformity of the atomic arrangement in this direction, the temperature depends only on the radial position ρ.

At small radius values, ρ < 1 nm, i.e. in the middle of the nanowire, the temperature is about constant. Then, at ρ > 2 nm, there is a steep decrease of the temperature towards the silicon-to-dioxide interface at ρ_{Si} = 2.6 nm. The decrease of the temperature continues also in the silicon dioxide layer. At the interface, a change in the slope of the curves is clearly visible.

To properly understand the role of radial heat transport from the nanowires, we will compare the absolute values of the thermal resistances for nanowires with the values typical

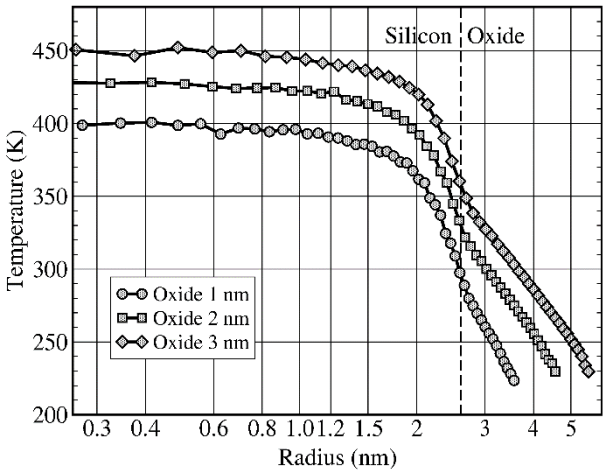

Fig. 5. Temperature distribution as a function of the radial position from the axis of the cylindrical nanowire. The radius of the silicon nanowire is 2.6 nm, the nanowire side wall is covered by silicon dioxide with a thickness of 1, 2, or 3 nm as indicated in the legend. The heat source power is 65.2 eV·ps^{-1}.

for applications in the CMOS technology. Accordingly, we also calculated the temperature distributions for the case of axial thermal transport. We varied the length of the nanowires and the thickness of the oxide on the silicon surface through which the heat transfer is established.

Fig. 6 shows axial temperature distributions for a silicon nanowire with a length of 11 nm covered on the end lids with an oxide layer of different thickness. The temperature profiles are qualitatively similar to the ones shown in the previous Fig. 5. The thicker the oxide is, the higher the maximum temperature and the lower the temperature at the boundary points of the curves. From the temperature distributions like the ones presented in Figs 5 and 6, thermal resistances for the heat transfer from the nanowires to external environment were calculated and the results are presented below.

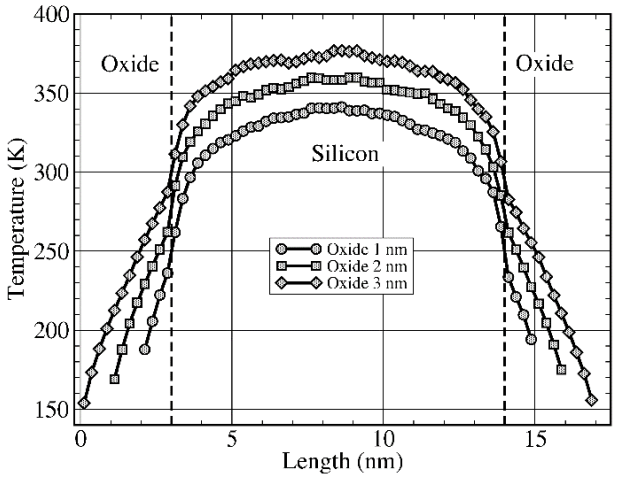

Fig. 6. Temperature distribution along the axis of the cylindrical nanowire with a length of 11 nm. The radius of the silicon nanowire is 2.6 nm, the nanowire top and bottom sides are covered by silicon dioxide with a thickness of 1, 2, or 3 nm as indicated in the legend. The heat source power is 15 eV·ps^{-1}.

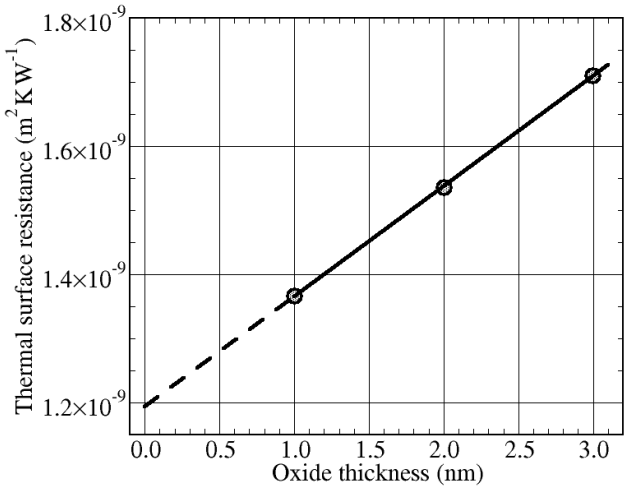

Fig. 7. Thermal surface resistance between the axis of the cylindrical silicon nanowire and the surface of the nanowire stack as a function of the silicon dioxide thickness covering the cylindrical side wall of the silicon nanowire.

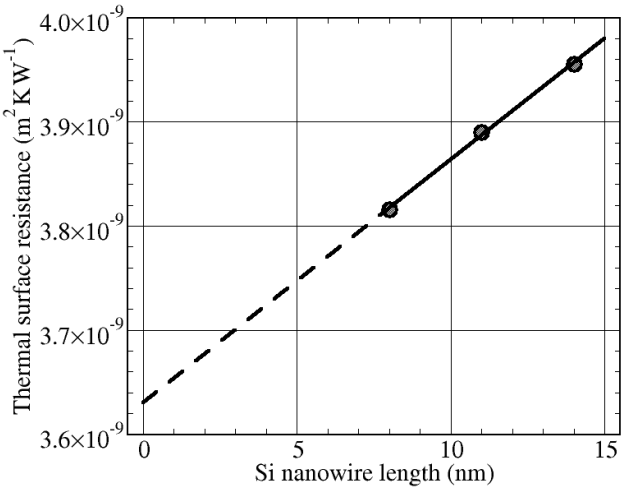

Fig. 8. Thermal resistance between the middle of the cylindrical silicon nanowires and the external top and bottom surfaces of the nanowire sample as a function of the silicon nanowire length. Thickness of the oxide covering the top and bottom sides of the silicon cylinders is 3 nm.

Fig 7 shows the thermal surface resistance R_{ths} as a function of oxide thickness for the radial heat transfer from the silicon nanowire to the outside of the oxide shell surrounding the nanowire as shown in Fig. 1. R_{ths} corresponds to the total thermal resistance multiplied by the area of the silicon surface through which the heat is transferred.

As demonstrated in Fig. 7, the radial thermal resistance increases linearly with the thickness of the oxide layer surrounding the silicon. This is qualitatively in accordance with the macroscopic thermal transport theory, but there are peculiarities for nanowires. First, in macroscopic theory the linearity holds for thin isolation layers $t_{ox} << \rho_{Si}$ only. Here, we have $t_{ox} = 3$ nm, and $\rho_{Si} = 2.6$ nm, but the linearity still holds. Then, if we extrapolate the value of R_{ths} to $t_{ox} = 0$, the R_{ths} for $t_{ox} = 0$ still has a considerable residual value of about $1.2 \cdot 10^{-9}$ m^2 KW^{-1}. This value is well comparable with the values of R_{ths} for oxide thicknesses in technologically relevant cases of $t_{ox} = 1$ to 3 nm. This residual value has two important contributions, the silicon-to-oxide interface resistance and the distributed resistance during the heat transport in silicon. Due to a strong impact of nano-size effects, which we demonstrated in Section 3, we could not separate these two contributions.

Fig.8 shows the axial thermal surface resistance R_{ths} in dependence on the nanowire length for the set-up in Fig.2. As for the radial heat transport, a linear dependence is observed. For a cylindrical silicon nanowire with $\rho_{Si} = 2.6$ nm and $L_{Si} = 10$ nm, a direct comparison of the values of the thermal resistances for radial and for axial transport in Table III shows that the resistances for the radial transport are about factor 3 to 4 lower than the resistances for axial heat transport along the <100>-oriented nanowire axis. This means that for the nanoscale structures investigated here, the radial heat transfer through the gate oxides can be more efficient than the axial heat transfer through the ends of the nanowires.

V. Conclusions

In conclusion, we have studied both radial and axial heat transfer in silicon nanowires surrounded by silicon dioxide using NEMD simulations. The results indicate a more intensive heat transfer in radial direction than along the axis.

TABLE III. Thermal Resistance to Heat Flow from the Uniformly Heated Cylindrical Silicon Nanowires through Thin Oxide Layers at the Lids to the Exterior

Direction of Heat transfer	Oxide Thickness (nm)	Silicon Nanowire Length (nm)	R_{th} (KW^{-1})
Radial	1	10	$1.67 \cdot 10^7$
Radial	2	10	$1.87 \cdot 10^7$
Radial	3	10	$2.09 \cdot 10^7$
Axial	1	10	$6.14 \cdot 10^7$
Axial	2	10	$7.75 \cdot 10^7$
Axial	3	10	$9.10 \cdot 10^7$

The observed deviation of the temperature distribution near the heat source in the silicon part of the locally heated nanowire from Fourier's law requires a further analysis.

[1] A. Boukai, Y. Bunimovich, J. Tahir-Kheli et al., "Silicon nanowires as efficient thermoelectric materials," Nature vol. 451, pp. 168–171, January 2008; A. Hochbaum, R. Chen, R. Delgado et al., "Enhanced thermoelectric performance of rough silicon nanowires," Nature vol. 451, pp. 163–167, January 2008.

[2] S. G. Volz, G. Chen, "Molecular dynamics simulation of thermal conductivity of silicon nanowires," Applied Physics Letters vol. 75 (14), pp. 2056-2058, October 1999.

[3] M. Verdier, Y. Han, D. Lacroix, P-O. Chapuis. and K. Termentzidis, "Radial dependence of thermal transport in silicon nanowires," J. Phys. Mater., vol. 2, pp. 015002(1-8), November 2019.

[4] A. Burenkov, V. Belko and J. Lorenz, "Self-heating of nano-scale SOI MOSFETs: TCAD and molecular dynamics simulations," 19th International Workshop on Thermal Investigations of ICs and Systems (THERMINIC), Berlin, 2013, pp. 305-308.

[5] S. Plimpton, "Fast Parallel Algorithms for Short-Range Molecular Dynamics," J. Comp. Phys., vol. 117, pp. 1-19, March 1995; http://lammps.sandia.gov

[6] S Munetoh, T. Motooka, K. Moriguchi, and A. Shintani, "Interatomic potential for Si-O systems using Tersoff parameterization," Comput. Materials Sci., vol. 39, pp. 334-339, 2007.

[7] W. Zhu, G. Zheng, S. Cao, H. He, "Thermal conductivity of amorphous SiO_2 thin film: A molecular dynamics study," Sci. Rep., vol. 8, pp. 10537(1-9), 2018.